Automated Analysis of ISO/IEC14443A Interrogator Command Pulse Shapes

Ulrich Muehlmann and Michael Gebhart
NXP Semiconductors Austria
Gratkorn, Styria, AUSTRIA
E-mail:ulrich.muehlmann@nxp.com, michael.gebhart@nxp.com

Abstract: **Conformity compliance tests are important measures to mitigate interoperability issues in open-loop RFID applications like e-Banking and e-Passport applications where interrogators and transponders are normally supplied by various different manufacturers. Timing evaluation is a crucial part of the conformance compliance tests. Therefore, it is necessary to have an exact evaluation method in place in order to avoid ambiguities and to reduce the degree of freedom in the interpretation of measurement results. A novel automated analysis of ISO/IEC 14443A interrogator command pulse shapes resistant to signal distortion is proposed in this manuscript. The envelope detector required is based on the Hilbert transform in the frequency domain. A theoretical analysis has shown that at least one base-band filter is required to reject phase noise and harmonic distortion on the signal envelope. Furthermore, the properties, especially the windowing effect, of the FFT and iFFT have to be taken into account to get proper results.**

1. INTRODUCTION

To ensure world-wide interoperability of products of different manufacturers, interrogators and transponders for e-Government and e-Banking applications have to perform according to International Standards. In this context, the Proximity Radio Frequency Identification Standard ISO/IEC14443 [10] is of particular importance. The total number of electronic e-Passports worldwide exceeds over 400 Million pieces so far. Therefore, interoperability issues have to be addressed carefully. Compared to several other applications in the field of Information Technology (IT), the ISO/IEC14443 RFID Standard is governed by the Joint Technical Committee 1 (JTC1), which combines the International Standards Organisation (ISO) and the International Electrotechnical Committee (IEC), in the Sub-Committee 17 (SC17), Working Group 8 (WG8) dealing with contactless integrated circuit cards (see [8] for details). The Product Standard describes and defines the properties of interrogators and transponders on the air interface for communication. In addition, the Test Standard ISO/IEC10373-6 [9] presents elementary hardware specifications for a contactless test setup (CTS) like a specific antenna arrangement, test methods and measurement procedures. Both standards are currently under revision, which means that several values and parameters as well as the measurement methods are under construction at the same time. The envelope parameters are crucial for the interrogator-to-transponder communication and can be the reason for interoperability issues. Therefore, one has to consider several different options of measurement and signal processing, should discuss pros and cons, and has to find out the most suitable method for this specific signal analysis. Due to the broad-band characteristics of 13.56 MHz proximity RFID Systems which used data rates up to 848 kbit/s and due to other physical and environmental effects, it is in fact important to use a method that is robust to noise and signal distortions. In this paper, we describe the extended air-interface measurement setup and discuss different approaches to determine these envelope parameters of the amplitude modulated (AM) 13.56 MHz carrier. The final method uses the Hilbert transform and a specific filter to achieve high noise immunity. A comparable implementation described in [1] is based on an empirical minimum-maximum approach which lacks of performance and accuracy. To our knowledge there is no other comparable automated analysis of ISO/IEC14443A interrogator command pulse shapes published in the literature which is resistant to signal distortion caused by the RFID measurement systems.

2. MEASUREMENT SETUP AND SIGNAL CHARACTERISTICS

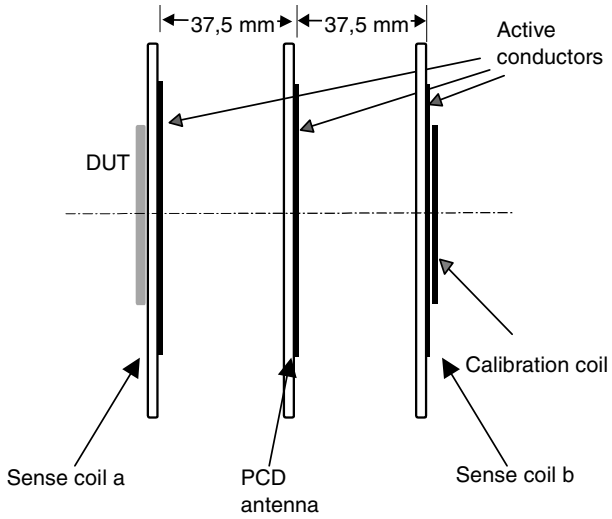

Figure 1 - Antenna arrangement for transponder test.

The Test Standard describes an antenna arrangement (as interrogator front-end emulation) for transponder tests. It

consists of a resonant loop antenna matched to 50 Ohm impedance and a Q-factor of about eight achieved with a specified network. The transponder as device under test (DUT) is placed in distance for homogenous H-field coaxial to the PCD antenna on one side, and a calibration coil for measurement of H-field by means of the induced voltage is placed on the opposite side. Load modulation of the DUT can be measured with two sense coils in symmetric Helmholtz arrangement, which compensates for the primary field of the PCD antenna and enables the measurement of the secondary field of the DUT only.

The resonant loop antenna distorts a modulated pulse in exponential decay and increase of the signal envelope edges, just like a real interrogator does. Modulation specified in the Product Standard considers this distortion and allows a range for each time parameter. ISO/IEC14443-2 specifies 4 time parameters and the residual carrier for Type A base data rate (106 kbit/s) and 3 time parameters and the residual carrier for higher data rates (HDR), to be measured at certain envelope amplitudes as shown in fig. 2. For Type B, the modulation index as well as rise and fall time are specified for all baud rates.

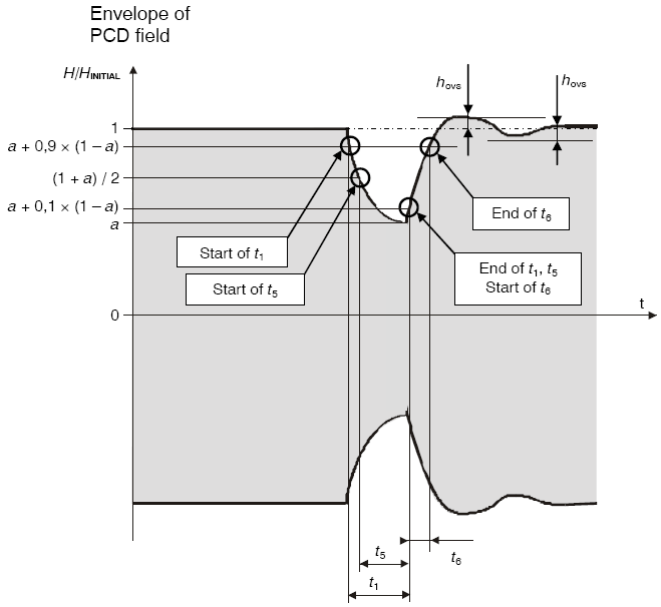

Figure 2 - ISO/IEC14443-2A HDR interrogator modulation evaluation and thresholds, taken from [10].

To be able to generate pulse shapes covering the full specified range for test, the antenna Q-factor should be rather low (to allow short time constants), and the antenna arrangement can be extended with an arbitrary waveform generator (AWG) for signal generation, which can be used to produce the modulated 13.56 MHz carrier as amplitude points over time, pre-conditioned to achieve any pulse shape in the specified range [1, 2]. Time constants of antenna and stored pulse shapes add up as the modulation parameters which are measured at the calibration coil (without DUT).

3. ENVELOPE DETECTORS

Some common envelope detection algorithms and its application to the given signal properties are discussed in this section. Let us start with the amplitude modulation principle according to a time domain signal *s(t):*

$$s(t) = [1 + m(t)]\cos(\omega_c t + \varphi), \tag{1}$$

where $m(t)$ is the base-band modulation signal, ω_c represents the angular carrier frequency, and φ is an arbitrary phase shift. Unfortunately, the modulation signal is mixed with a carrier that in reality features noise and harmonics, therefore we can write:

$$s(t) = [1 + m(t)]\sum_{k=0}^{n} A_k \cos(k\omega_c t + \varphi_k) + w(t), \tag{2}$$

where A_k and φ_k define the amplitude value and phase, k is the number of every single harmonic component, and $w(t)$ represents the noise term.

3.1 Envelope Detection based on Hilbert Transform

For every single term of equation 2 we can write the time to frequency domain relation as:

$$\begin{aligned} &v(t)\cos(k\omega_c t + \varphi_k) \leftrightarrow \\ &\frac{e^{j\varphi_k}}{2}\underline{V}(\omega - k\omega_c) + \frac{e^{-j\varphi_k}}{2}\underline{V}(\omega + k\omega_c), \end{aligned} \tag{3}$$

where $v(t)$ represents the baseband modulation signal and $V(\omega)$ is the Fourier transformation of $v(t)$, k and ω_c reflect the k-th harmonics and the angular carrier frequency of the fundamental wave, and φ_k formulates the phase relation. Next, we can derive the Hilbert transform by starting with its corresponding multiplicative operator in the frequency domain known as:

$$F\left\{\frac{1}{\pi t}\right\} = -j\,\mathrm{sgn}(\omega) = e^{-j\frac{\pi}{2}\mathrm{sgn}(\omega)}, \tag{4}$$

where $F\{\}$ denotes the Fourier transformation, and t, ω are the time-domain and frequency domain variables, respectively.

By using the Hilbert transform on every single component in the frequency domain and back-transformation to the time domain we obtain:

$$\begin{aligned} &\frac{e^{j\varphi_k}}{2}\underline{V}(\omega - k\omega_c)e^{j\frac{\pi}{2}} + \frac{e^{-j\varphi_k}}{2}\underline{V}(\omega + k\omega_c)e^{-j\frac{\pi}{2}} \leftrightarrow \\ &v(t)\cos(k\omega_c + \varphi_k + \frac{\pi}{2}) = -v(t)\sin(k\omega_c + \varphi_k) \end{aligned} \tag{5}$$

Appling this to the entire signal group we get:

$$\begin{aligned} s(t) &= [1 + m(t)]\sum_{k=0}^{n} A_k \cos(k\omega_c t + \varphi_k) + w(t) \\ s_H(t) &= -[1 + m(t)]\sum_{k=0}^{n} A_k \sin(k\omega_c t + \varphi_k) + w(t), \end{aligned} \tag{6}$$

where $s(t)$ is the analytical or measured signal group and $s_H(t)$ is the 90° shifted signal group as the output of the Hilbert transform. Finally, the base-band amplitude, also referred to as the envelope of the carrier signal, is derived with:

$$a(t) = \sqrt{s(t)^2 + s_H(t)^2}. \tag{7}$$

By inserting $s(t)$ and $s_H(t)$ of eq. 6 in eq. 7 we get:

$$a(t) = [1 + m(t)] \sqrt{\left[\sum_{k=0}^{n} A_k \cos(k\omega_c t + \varphi_k)\right]^2 + \left[\sum_{k=0}^{n} A_k \sin(k\omega_c t + \varphi_k)\right]^2} + w(t). \tag{8}$$

In the ideal case, when only the fundamental wave of the carrier signal is present, we obtain

$$a(t) = [1 + m(t)] \sqrt{\cos(\omega_c t)^2 + \sin(\omega_c t)^2} = [1 + m(t)] \tag{9}$$

as the base-band component. Without loss of generality, we just describe the case when the third and fifth harmonics in addition to the fundamental wave are present as:

$$a_{3,5}(t) = [1 + m(t)] \sqrt{\begin{aligned} &16A_1A_5\cos(\omega_c t)^4 + \\ &+ (4A_1A_3 - 16A_1A_5 + 4A_3A_5)\cos(\omega_c t)^2 + \\ &+ A_1{}^2 + A_3{}^2 + A_5{}^2 - 2A_1A_3 + \\ &+ 2A_1A_5 - 2A_3A_5 \end{aligned}} \tag{10}$$

Another typical example in reality reflects the case when the fundamental wave, the second and third harmonics are present as:

$$a_{2,3}(t) = [1 + m(t)] \sqrt{\begin{aligned} &4A_1A_3\cos(\omega_c t)^2 + \\ &+ (2A_1A_2 + 2A_3A_2)\cos(\omega_c t) + \\ &+ A_1{}^2 + A_3{}^2 - 2A_1A_3 + A_2{}^2 \end{aligned}} \tag{11}$$

It can be noted that: If harmonics are present in the carrier signal one will discover some sort of oscillation including an undesirable offset shift on the extracted envelope signal. As pointed out in [3, 13], when the Hilbert transform is based on the FFT transformation, amplitude and phase fluctuations, leakage and picket fence effect, and windowing-effects have to be taken into account.

3.2 Envelope Detection based on IQ Demodulation

In the normal measurement setup condition, it will not be possible to perform a synchronous down conversion since the data is captured by means of an oscilloscope and post-processed offline in the digital domain. IQ demodulation is used to extract the baseband signal in order to be resistant against phase variations and to preserve the desired amplitude values. The basic derivation of IQ demodulation can be found in [7]. We just present the results when the second and third (eq. 12), the third and fifth harmonics (eq. 13) are present. The B_i terms are combinations of A_1 to A_3 or A_1 to A_5.

$$a_{2,3}(t) = [1 + m(t)] \sqrt{\frac{A_1^2}{2} + \frac{A_2^2}{2} + \frac{A_3^2}{2} + \sum_{i=1}^{6} B_i \cos(i\omega_c t)} \tag{12}$$

$$a_{3,5}(t) = [1 + m(t)] \sqrt{\frac{A_1^2}{2} + \frac{A_3^2}{2} + \frac{A_5^2}{2} + \sum_{i=1}^{5} B_i \cos(2i\omega_c t)} \tag{13}$$

It has to be noted that by using IQ demodulation as envelope detector a low-pass filter has to be applied in any case since the 2nd harmonics will always be a residual mixing product even if no distortion on the carrier signal is present. This can be seen as a drawback in comparison to the Hilbert transform approach. Furthermore, all the harmonic components will contribute to the amplitude of the extracted baseband signal $m(t)$.

3.3 Envelope Detection based on Squaring and Low Pass-Filtering

Envelope detection based on squaring and low pass-filtering is a standard procedure of applied signal processing (see [7] for details). According to 3.1, we present just the results of the second and third, and third and fifth harmonics on the carrier signal and its influence on the envelope's shape.

$$a_{2,3}(t) = [1 + m(t)] \left(\frac{A_1^2}{2} + \frac{A_2^2}{2} + \frac{A_3^2}{2} + \sum_{i=1}^{6} B_i \cos(i\omega_c t) \right) \tag{14}$$

$$a_{3,5}(t) = [1 + m(t)] \left(\frac{A_1^2}{2} + \frac{A_3^2}{2} + \frac{A_5^2}{2} + \sum_{i=1}^{5} B_i \cos(2i\omega_c t) \right) \tag{15}$$

It can be seen that the results are similar to the IQ-demodulation method. In addition to a low pass filter that rejects the harmonic components, an appropriate constant amplitude gain correction factor has to be applied to compare all the results of the present envelope detectors.

3.4 Selection of the Optimum Envelope Detector for the Present Problem Formulation

Basically, all presented envelope detectors are capable of extracting the modulation sequence $m(t)$, whereas IQ and squaring based approaches require an image rejection filter of components located on $2\omega_c$, even if no distortion affects the signal amplitude. The Hilbert transform based approach is selected for the present problem formulation. One reason emerges from the fact that this envelope detector was already presented as the de-facto standard several years ago by the ICAO/BSI conformity standardization bodies [11, 12]. The second reason is associated with the property of the Hilbert

transform. It gives exact results on amplitude modulated carriers having one single frequency and no phase noise. But in reality, it is crucial to apply appropriate filters to cancel the harmonic components and to minimize phase noise issues in order to gain a valuable estimate of the actual signal envelope.

4. BASE-BAND FILTER DESIGN

The proposed automated analysis will be performed in the digital domain. The sampling rate is set to 500 Msps. This is a tradeoff between the number of amplitude points per wave-length of the fundamental wave ω_c and the angular resolution of the Hilbert transform, and the number of filter coefficients of the base-band finite impulse response (FIR) filter. An infinite impulse response (IIR) would be easier to implement but its non-constant group delay will affect the timing evaluation of the modulated signal amplitude *m(t)*. A minimum-order, equiripple filter design method [4, 5, 6] is used to determine the filter coefficients of the proposed filter. As an outcome of eq. 3 to 11 in the presence of harmonic distortion, a low pass filter will be required. Unfortunately, the phase noise of the fundamental wave cannot be filtered in advance since it carries the information of the modulation signal *m(t)*. This means that two filter stages are required, one low-pass filter to filter all the harmonics and one smoothing filter after the envelope detection to filter the phase noise of the fundamental wave ω_c. We combine the low-pass filter and the smoothing filter and add the filtering procedure as the final stage after Hilbert transform and absolute value (eq. 7) calculation. This will introduce an additional gain value according to eq. 10 and 11 which does not influence the timing evaluation, because the amplitude is normalized as illustrated in fig. 2. The applied filter is characterized by a transition area between pass-band and stop-band which is 6 MHz wide starting at 7 MHz and ending at 13 MHz. These settings allow base-band signals up to 7 MHz and do not cancel fast transitions of the modulation signal amplitude.

5. MEASUREMENT AND EVALUATION RESULTS

For the measurement setup a digital arbitrary wave-form generator (AWG) based on a FPGA with post connected DAC is used. The analog signal is amplified by means of a commercially available power amplifier AR75X200. The amplified signal is applied to the antenna arrangement illustrated in fig. 1 and an oscilloscope is connected to the calibration coil output as defined in [10] to measure the PCD field strength and its waveform. A typical automated measurement and evaluation result is illustrated in fig. 3 at 106kbit/s data-rate and fig. 4 at 424 kbit/s data-rate on a 13.56 MHz carrier.

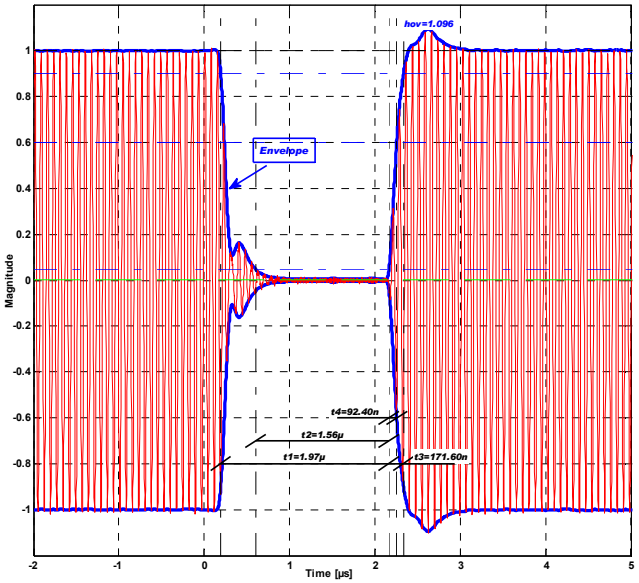

Figure 3 - ISO/IEC14443-2A interrogator modulation measurement and evaluation based on the proposed envelope detection and filtering method, data rate 106 kbit/s, type A.

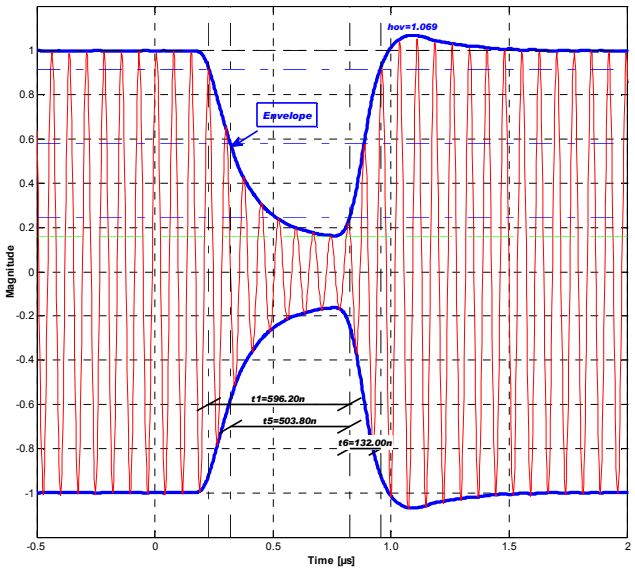

Figure 4 - ISO/IEC14443-2A interrogator modulation measurement and evaluation based on the proposed envelope detection and filtering method, data rate 424 kbit/s type A.

As already mentioned, the Hilbert transform is applied in the frequency domain and is based on FFT and iFFT transformation accordingly. The implementation referred to fig. 3 and fig. 4 avoids the additional convolution of the rectangular window function emerging from the acquired sample set which is finite. The acquired sample set can be easily made finite for the FFT function by truncation of some last samples to appear the continuous sample set sequence to be infinite without discontinues in the carrier signal. Windowing functions in the time domain are not applicable due to amplitude fluctuation of the base-band signal after back-transformation and complex magnitude calculation.

In contrast, Fig. 5 shows the envelope analysis of a Standard compliant waveform without base-band filter and without pre-conditioning for the FFT as discussed before. The hard magnitude thresholds defined by the Standard (refer to Fig. 2) will result in a false timing analysis which can mistake the DUT for a device with interoperability issues.

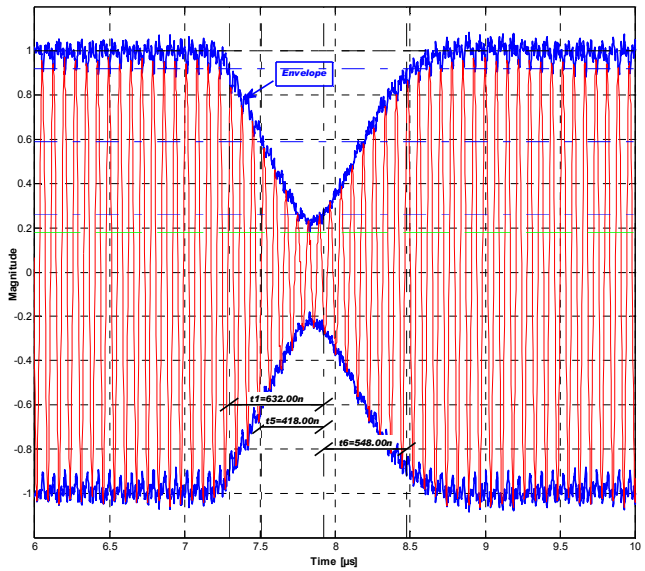

Figure 5 - Envelope extraction without filter and proper windowing

6. CONCLUSION

In this paper a proper envelope detection algorithm is proposed for an automated ISO/IEC14443A interrogator command pulse shape analysis. The algorithm is based on the Hilbert transform in the frequency domain. A carefully selected sample set as well as at least one base-band filter with constant group delay characteristics is required in order to overcome distortion and FFT/iFFT transformation issues. A proper implementation of the envelope detector as well as the selection of the base-band filter is important for the given signal characteristic. Even the hard amplitude thresholds where the timings are extracted can cause false positive interoperability issues when these requirements are not taken into account.

REFERENCES

[1] M. Gebhart, M. Wienand, J. Bruckbauer, S. Birnstingl: "Automatic Analysis of 13.56 MHz Reader Command modulation pulses", 2nd EURASIP Workshop on RFID Technology, Budapest, 2008.

[2] M. Gebhart, S. Birnstingl, J. Bruckbauer, E. Merlin: "Properties of a test bench to verify Standard Compliance of Proximity Transponders", 6th International Symposium on Communication Systems, Networks and Digital Signal Processing (CSNDSP), pp. 306-310, Graz, Austria, 2008.

[3] D. Shi, P.J. Unsworth, R.X. Gao: "Sensorless speed measurement of induction motor using Hilbert transform and interpolated fast Fourier transform", IEEE Transactions on Instrumentation and Measurement, Vol. 55, Issue 1, pp 290-299, Feb 2006.

[4] D.J. Shpak, and A. Antoniou: "A generalized Remez method for the design of FIR digital filters", IEEE Transactions on Circuits and Systems, pp. 161-174, 1990.

[5] A.V. Oppenheim, and R.W. Schafer: "Discrete-Time Signal Processing", Prentice-Hall, Englewood Cliffs, NJ, pp. 256-266, 1989.

[6] L.R. Rabiner, J.H. McClellan, and T.W. Parks: "FIR Digital Filter Design Techniques Using Weighted Chebyshev Approximations", Proceedings of the IEEE, Vol. 63, 1975

[7] J. G. Proakis: "Digital Communications", 2nd edition, New York: McGraw Hill, 1989.

[8] International Organization for Standardization (ISO): "Summary of SC17 standards", 2005, www.sc17.com

[9] International Organization for Standardization (ISO): "Identification Cards - Test Methods - Part 6: Test Methods", ISO/IEC 10373-6, 2001.

[10] International Organization for Standardization (ISO): "Identification Cards - Contactless integrated circuit(s) cards - proximity cards - Part 2: Radio Frequency power and signal interface", ISO/IEC FCD 14443-2: 2008, 14443-3:2009.

[11] BSI: "Testplan for ICAO compliant PCD Layer 2-4", Technical Report: TR-03105, 2008.

[12] International Organization for Standardization (ISO): "Test methods for ePassport", ISO/IEC 10373-6:2001 FPDAM7, Annex N, Working group document, not publicly available.

[13] F. Xaver: "Envelope detector based on Hilbert transform", Diploma thesis, Institute of Communications and Radio-Frequency Engineering, Vienna University of Technology, Austria, 2009.